Int J Syst Assur Eng Manag
https://doi.org/10.1007/s13198-023-02061-5

ORIGINAL ARTICLE

Optimal control of output power of micro-inverter based on circuit design

Pu Cheng[1]

Received: 15 March 2023 / Revised: 20 June 2023 / Accepted: 19 July 2023

Abstract In the context of energy shortage and increasingly serious security problems in the world, the utilization of renewable energy has attracted much attention. This paper studies the maximum limit of grid-connection, starting from the integrated control strategy of single stage photovoltaic grid-connection system, using the mathematical model and method of solar cell array. And the topological structure of the single-stage photovoltaic power generation (pv) grid system, based on the system in mathematics The research modem proposes a variable step MPPT algorithm and decides the integrated control strategy of the single-stage photovoltaic grid-connected system. Finally, combined with industrial practical applications, this article provides a single-stage grid-connected solar power system based on RTW limited EatTimworks technology TMS 320 F 28,335 series DS, which improves the realization of the hardware circuit and the stability of the single-stage photovoltaic grid-connected system. This article will analyze and compare the topological structure of two single-stage photovoltaic grid-connected systems. Based on the decision of the bipolar topology, the overall control method of the system is explained, and the advantages and disadvantages of the two overall control methods are pointed out. Then, establish a photovoltaic simulation model to display the output characteristics of the photovoltaic array, analyze and compare the three commonly used MPPT tracking methods, adopt a variable step integrated MPPT tracking control method, show the advantages of this method, and verify it through simulation. Finally, this article describes the outline of the voltage and current-based double closed-loop grid-connected inverter control strategy, establishes the corresponding mathematical model, and analyzes and analyzes the three commonly used full-bridge inverter SPWM modulation modes through simulation. Compared.

Keywords Unipolar photovoltaic · Grid-connected algorithm · Micro-inverter · Output power optimization

1 Introduction

Due to the increase of human awareness of environmental protection and the exhaustion of non-renewable energy, photovoltaic grid-connected power generation has become an important green energy source in the 21st century (Balaguer et al. 2010). Single-phase grid-connected solar power inverters are widely used on the roof of buildings and have great application possibilities. The quality of these output currents will directly affect the power grid and users. This paper studies the output power control strategy of single-phase solar power inverters(Kabalcı 2020). First, analyze the topological structure of the single-phase inverter, and design the topological structure of the secondary single-phase transformer as the research object of this thesis (Kumar and Fernandes 2017). Next, based on the mathematical model of solar cells, in order to improve the maximum power point following (MPPT) speed and reduce power vibration, a variable step perturbation observation method is proposed. In recent years, during the rapid development of the national economy, energy has always been one of the important development foundations (Pfenninger et al. 2014). With the progress of social science and technology and the increase of population, the world's energy demand is increasing rapidly, causing the problem of energy shortage. On the other hand,

✉ Pu Cheng
20160412@ayit.edu.cn

[1] Hebei Chemical and Pharmaceutical College, Shijiazhuang 050026, China

Published online: 04 August 2023

in recent years, the global ecological environment has seen undesirable phenomena such as environmental pollution, ecosystem deterioration, and global warming. Because of this series of issues, people basically reached an agreement on energy issues (Fiaschi et al. 2012). In other words, the development of new energy and renewable energy, the realization of sustainable economic development, and the development of support policies for new energy development by governments around the world. New energy power generation includes solar power generation, wind power generation, micro gas turbines, fuel cells, and biomass power generation (Zhao and Chen 2018). The solar power mentioned in this article is a power generation technology that uses solar radiation. Because it has a wide range of distribution, a large number, can be reused, and is green and environmentally friendly, it is widely promoted worldwide (Barlev et al. 2011). Based on this, this article describes the current status of research and use at home and abroad. Foreign countries, European and American countries have already launched corresponding promotion plans, and Japan has also followed up with new energy use plans (Guerrero et al. 2010). Up to now, the global new plan has reached the United Nations power generation and grid-connected installed capacity of 150,000 photovoltaics, but the world's total equipment The capacity is less than 1% (Schot et al. 2016). By 2030, the world's solar power generation equipment capacity will reach 300GW, and the output value of the entire industry may exceed 300 billion U.S. dollars. By 2040, solar power generation will account for 15-20% of the world's electricity generation. According to this plan, the compound growth rate of the solar power generation industry from 2010 to 2040 will reach 25%. Among them, the development of grid-connected applications has been further advanced, forming three main application areas: grid-connected power generation (about 46%), off-grid power generation (about 27%), and communication base stations (about 27%).

2 Related work

The literature firstly analyzes and compares two single-phase solar grid-connected power generation systems. Based on the choice of bipolar topology, the overall control method of the system is explained, and the advantages and disadvantages of the two comprehensive control methods are explained systematically (Hill2012;Chiu 2010]. The literature points out that in the past 20 to 30 years, solar power generation technology has been continuously developed, and solar power grids have become one of the main methods of using solar energy. The research on the grid-connected solar power inverter system is of great practical significance in theory and practice for alleviating energy and environmental problems, researching and developing high-performance decentralized power generation systems, expanding the broad solar power market, and learning advanced technologies in related fields (Chiu 2010; Wu and Chou 2013). The literature proposes an engineering model based on the basic parameters of photovoltaic modules, the number of modules in series and parallel in the photovoltaic array, and the actual lighting temperature conditions(Kouro et al. 2015). According to the research and analysis of the mathematical model of the solar power generation array in the literature, in order to enable the solar power generation array to accurately reflect the influence of any lighting and temperature, the voltage, lighting and temperature parameters of the simplified engineering model have been adjusted. According to the analysis of the output characteristics of the solar cell array, in order to maximize the utilization of the output power of the solar cell array, a stable output power array is used(Kumari and Babu 2012). The most commonly used maximum output methods include constant voltage method, short-circuit current method, external interference observation method, and conductance increment method. In order to overcome the problems of vibration and misjudgment, several control methods such as optimal gradient method, stage approximation method, hysteresis comparison method, power prediction method, and central difference method are proposed (Abadie et al. 2010).

There is a positive and negative sequence current tracking control method based on positive and negative double coordinate system, and a control strategy that completely eliminates voltage harmonics using symmetric component method (Wang et al. 2019). The prerequisite for precise control on the DC side is the correct detection and separation of positive and negative sequence components. The delay method is simple to implement and can correctly separate the positive and negative sequence components, but it is sensitive to the harmonics of the power network and the system has a long delay time. The law of notch can solve this problem well. The literature has a lot of research literature on micro-photovoltaic inverters. This section mainly focuses on the research of micro-inverter topology. According to the micro-reverse series classification, it can be divided into single-stage, two-stage, and multi-stage inverters (Keshani et al. 2018). According to the presence or absence of a transformer, it can be divided into insulated fine-tuning burners and non-insulated fine-tuning burners. According to the type of DC bus, it can be classified into DC bus type, pseudo DC bus type, and non-DC bus type. The literature ranges from the circuit design of flyback micro-inverters, control algorithm and controller design, MPPT algorithm research, grid-connected current control, islanding detection, output filter design, power decoupling, efficiency calculation and optimization. In addition to the research on the flyback structure, there are many literatures on the topology of the flyback micro-inverter, which have derived forward and

flyback micro-inversion, dual-tube micro-inversion, and two-way micro-inversion based on flyback circuits (Rezaei2015; Yaoob2021]. Numerous structures. The literature proposes an active clamp soft switching circuit for interleaved parallel flyback micro-inverters, which can solve the leakage inductance problem of the transformer, reduce the energy loss caused by the leakage inductance, and reduce the switching tube turn-off voltage spike. It is proposed to use the negative half-cycle grid current to discharge the parasitic capacitance of the primary side MOS, so as to realize the zero voltage turn-on of the primary side MOS. It is proposed that the flyback micro-inverter adopts synchronous rectification technology. A quasi-resonant control strategy realized by a differential circuit is proposed for the staggered parallel flyback micro-inversion. For three-phase micro-inversion, a dynamic dead zone control technology and a phase skipping control strategy are proposed. A ZVS control strategy is proposed for forward and flyback circuits. A quasi-resonant dual-tube flyback micro-inverse topology is proposed. Mainly by improving the reference value of the current peak value under DCM/BCM/CCM to improve the efficiency of the flyback micro-inversion from the perspective of control. The application in the flyback micro-inversion is analyzed.

3 Design of optimal control algorithm model for output power of unipolar photovoltaic grid-connected micro-inverter

3.1 Grid-connected power generation algorithm

Solar panels are a type of solar system that realizes photovoltaic conversion. The voltage is generated by the photovoltaic effect under light conditions. The open circuit voltage of each solar cell is the same under the same lighting and temperature conditions. By connecting multiple cells in series, solar panels with specific parameters can be formed. In general, the sequence and parallel parameters of the panel are as follows.

It is assumed that the open circuit voltage of each solar cell unit is the rated power. The system assumes that the input voltage is U, and the number of panels in series is as follows:

$$\mathrm{M} = \mathrm{U}/u_0 \tag{1}$$

The number of units connected in parallel on each string of battery arrays:

$$N = P/(M * P_0) \tag{2}$$

After configuring the solar panels, you can select the relevant parameters such as the input voltage and rated power of the photovoltaic grid-connected inverter based on this.

Starting from Fig. 1, since the characteristic curve of the solar cell is non-linear, the output power of the solar panel inverter is detected in real time, and finally it runs at the maximum power.

The incremental conductance method is based on the power derivative of the maximum power tracking voltage. So it looks like this:

$$\mathrm{dP/dU} = \mathrm{I} + (\mathrm{U}*\mathrm{dI/dU}) = 0 \tag{3}$$

$$\mathrm{dI/dU} = -\mathrm{I/U} \tag{4}$$

Let C=−I/U, $C = dI/dU$, then:

When C=C, the panel runs at the maximum power point. When C > C, the panel works on the left side of the maximum power point. To increase the output power, it is necessary to increase the operating voltage of the panel. Therefore, in order to determine the direction of change of the operating voltage of the panel to perform MPPT, however, because the control algorithm requires high-precision system sampling and control, the installation will be more complicated.

In this paper, MPPT is accomplished by perturbing the voltage with a variable step length. Although the single-stage system voltage cannot directly control the panel, by adjusting the output grid current of the full-bridge inverter circuit to control the system, the output power of the solar cell can be changed, thereby changing the operating point voltage of the panel, and then comparing the power adjustment changes. Before and after, determine the control voltage for the next cycle in which the direction is changed. Therefore, adjust the size of the grid-connected current.

The output power of the solar panel is:

$$\text{Pool Power} = \text{Pool Volt}*\text{Pool Curr} \tag{5}$$

Next, the output voltage difference between 2 sampling periods is calculated as follows:

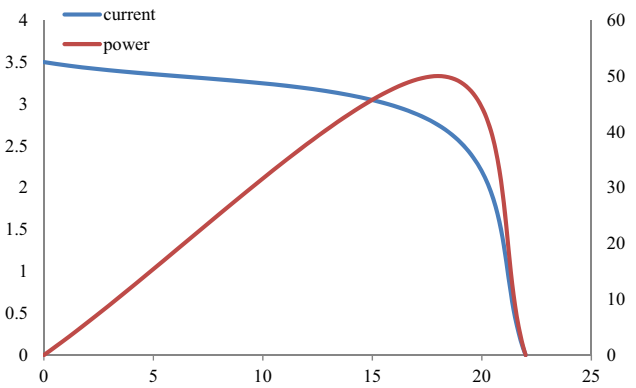

Fig. 1 Solar cell characteristic curve

$$\text{Delta volt} = \text{Pool Volt} - \text{Last Volt} \tag{6}$$

The output power difference between two sampling periods is:

$$\text{Delta power} = \text{pool power} - \text{Last Power} \tag{7}$$

Then the product of the two differences is:

$$\text{Power Volt} = \text{delta volt*delta power} \tag{8}$$

It can be seen from the P-U characteristic curve that in order to improve the output power, the output voltage of the panel needs to be increased.

$$\text{Uerf} = \text{pool volt} + \text{Volt\_Step} \tag{9}$$

Among them, *Uerf* is the expected voltage, and *Volt_Step* is the voltage improvement. Similarly, when *PowerVolt*<0, there are:

$$\text{Uref} = \text{pool volt} - \text{Volt\_Step} \tag{10}$$

Generally speaking, the maximum power point voltage is about 80% of the panel open circuit voltage. Then, when the panel voltage is between U1 and U2, the smaller step size S_Step, when it exceeds this range, the larger step size L_Step is selected.

As shown in Fig. 2, when the lighting is reduced sharply, the system can reduce the output grid-connected current within a time, so the energy of the front and back stages of the system is balanced. Therefore, after the bus voltage drops, it will be adjusted to a stable state immediately to avoid bus collapse.

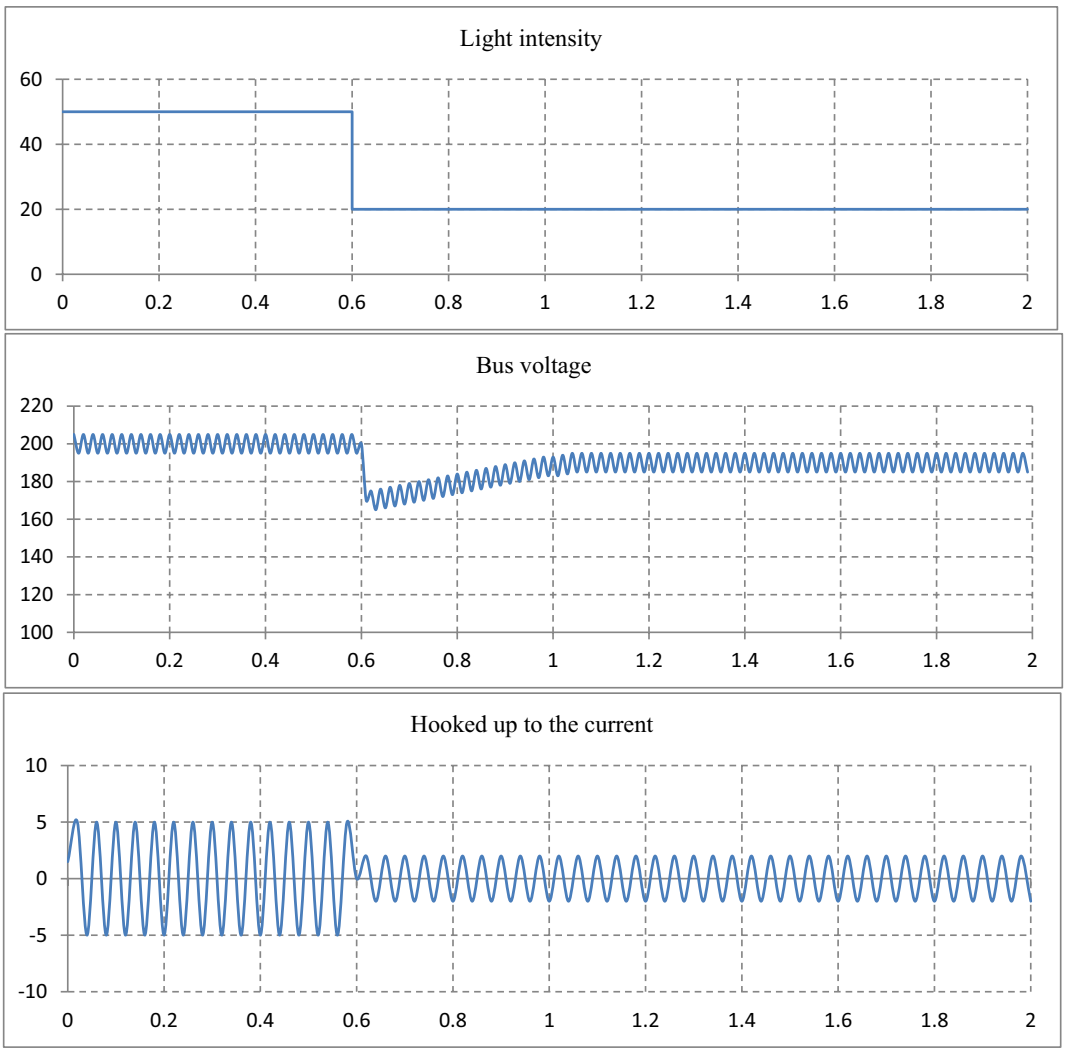

Fig. 2 MPPT customer service bus crashes

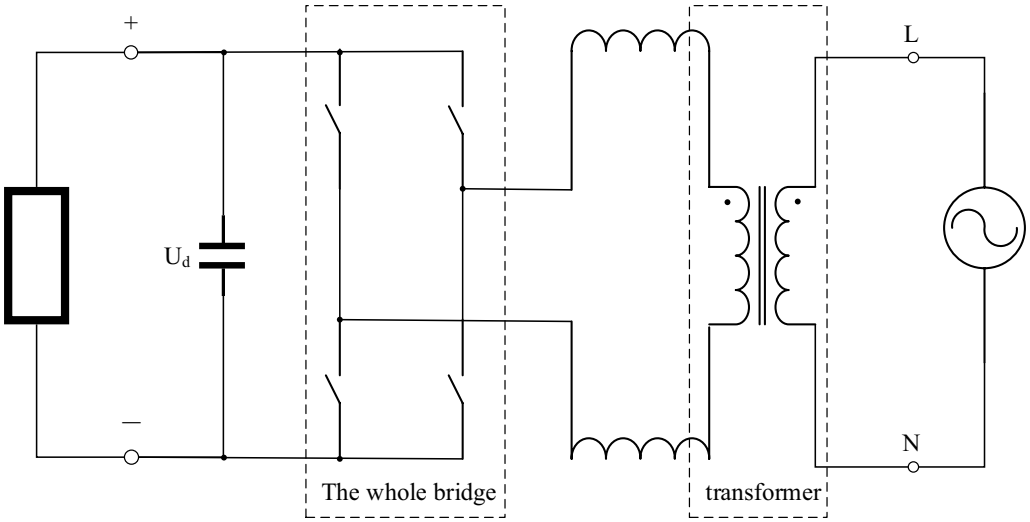

Fig. 3 Typical unipolar topology

3.2 Micro-inverter design

Starting from Fig. 3, the circuit of this scheme is a simple, low-cost sampling and power supply system. It is not the front end of the interconnection transformer DC, but the end of the electrical insulation connected to the insulating transformer, power grid and frequency converter. In power grid components, system security is good, but power frequency transformers will increase cost, capacity, and weight, resulting in energy loss. From the point of view of current transmission, the DC side of the bridge is lower, and the current flowing through the bridge is larger, so the loss of the switch tube is larger. Therefore, the energy conversion efficiency of the system is reduced. Therefore, in order to improve system efficiency, it is necessary to improve the control method.

The control goal of the inverter system is to synchronize the output of the current connected to the grid with the power grid, so that the system always outputs at maximum power. In the single-stage topology used in this system, the transformer only plays the role of voltage boost and electrical insulation. Since the output voltage of the inverter is fixed, the grid-connected current determines the output power. Generally speaking, the energy before and after the capacitor of the inverter bus is saved. Therefore, by controlling the full bridge connection, the grid-connected current can be changed, so the basic solar output power of the single-stage inverter maximum power tracking can be changed.

As shown in Fig. 4, the positive output pole and the negative output pole of the solar panel are respectively connected to DC + and DC−. The bus capacitor connects the input and the inverter bridge, and uses the energy storage function of the bus capacitor to buffer the power balance of the front

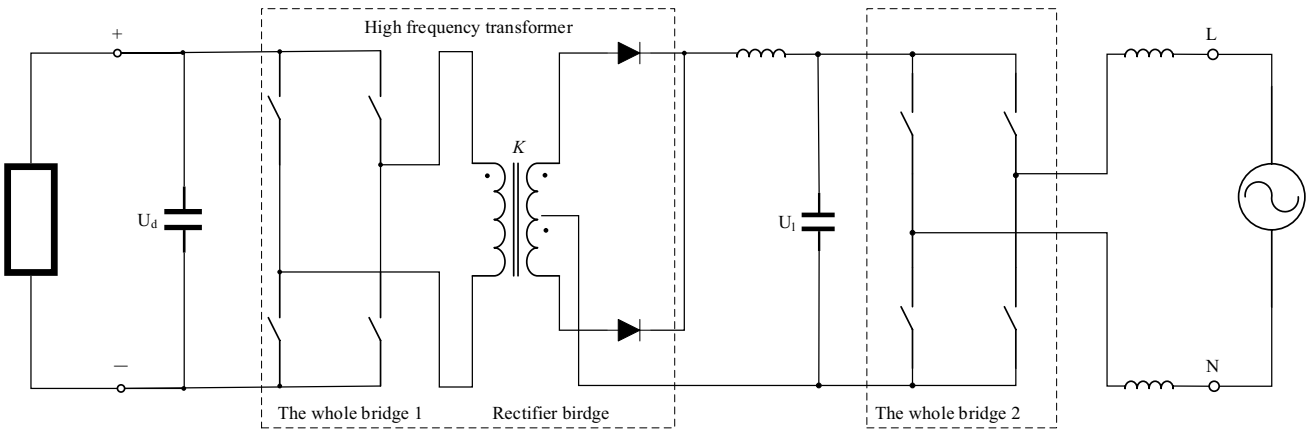

Fig. 4 Power system hardware structure

and rear stages. The full bridge circuit is the core circuit of the system, which completes the maximum power tracking and inverter link. The bridge arm is composed of 4 fully controlled power switches (IGBT). The full-bridge high-frequency modulation outputs high-frequency square wave signals, and each output is connected to a grid-connected inductor to filter 50 Hz signals. In order to increase the voltage and achieve insulation between the power grid and the inverter, a power frequency transformer of 1:2.5 was selected. The capacitor connected to the grid-connected inductor through the back end of the transformer can form a secondary filter. As a result, the grid-connected current waveform becomes smooth and meets the requirements of the power grid. By connecting two-stage grid-connected relays in series, the reliability of the system can be improved.

3.3 Output power optimization control algorithm

Each solar cell module in the system is equipped with an independent power optimizer. The core of the power oscilloscope is DC. The input terminal is connected with the solar cell module, and the output terminal is connected in series, as the input of the rear grid-connected inverter to form the DC converter of the DC bus. Each power oscilloscope adjusts the output voltage of the connected PV module through an independent MPPT module, so that each PV module operates at its own maximum power point (MPP). The MPPT module does not require a later grid-connected inverter. Its main function is to balance the energy incorporated into the grid through the energy generated by all solar power modules in the system and the inverter, and maintain stability to become a DC bus.Voltage. Even if an electric optical drive is added, the difference between PV modules is not considered. When the PV modules in the system receive the same amount of light, the generation of the system will not increase. Taking into account these undesirable conditions, you can increase the energy output of the system by adding a power calculator to the system.

If the system is in a stable state and the lighting will not change, the total power generated by all power oscilloscopes can be expressed as follows:

$$P_{tot} = \sum_{i=1}^{N} \left(V_{out,i} I_{out,i} \right) \tag{11}$$

Here, the output voltage and current refer to the number of series power oscilloscopes in the system. The total DC bus voltage ‰ can be expressed as follows:

$$V_{bus} = \sum_{i=1}^{N} V_{out,i} \tag{12}$$

In the steady state, the output current of each power calculator is equal, so the following information can be obtained:

$$I_{out,i} = I_{out,j} = I_{bus} \tag{13}$$

The output voltage of each power display can be expressed as follows:

$$V_{out,i} = \frac{P_{out,i}}{P_{tot}} * V_{bus} \tag{14}$$

Considering the withstand voltage of the switchgear, the output voltage must be limited within a specific range. Under different lighting conditions, the maximum power of the solar power generation module does not change much, so based on the input voltage ‰ of the power oscilloscope, the output voltage can be expressed as follows:

$$V_{out,i} = k_i * V_{mpp}, k_{min} \le k_i \le k_{max} \tag{15}$$

Here k_i is the voltage ratio of the i-th power calculator, and k_{min} and k_{max} are the minimum and maximum values, respectively. The range of island values is determined by the topology originally adopted by the power calculator. When the power optimina uses Buck circuit, then k_{max}=1, when the power oscilloscope uses Boost circuit, k_{max}=1.

The maximum power point voltage of the solar power generation module is basically unchanged even if the tracker or lighting changes. If it is assumed that it is only affected by the output current of the solar power generation module, the input power of the power optimina can be expressed as follows:

$$P_{mpp,i} = V_{mpp} * \left(\alpha_i * I_{mpp} \right), 0 \le \alpha_i \le 1 \tag{16}$$

Here, α_i represents the degree to which the solar cell module is completely shaded, and α_i==0 means that the solar cell module is completely shaded. If you ignore the loss of the power automata, you can get the output current of the power automat as follows:

$$I_{out,i} = \alpha_i * I_{mpp} / k_i \tag{17}$$

The output currents of all power calculators are equal, so the above equation can be further simplified:

$$\frac{\alpha_i}{k_i} = \alpha_j / k_j \tag{18}$$

Taking into account the working conditions, the system may contain N solar cell modules. Among them, the maximum power point current of the unshaded solar cell module and the voltage variation ratio of the power oscilloscope are as follows. The maximum power is m points. According to the above conditions, it can be simplified as follows:

$$k_m = \alpha * k_n \tag{19}$$

Let the $\beta = n/N$, DC bus voltage V_{bus} be expressed as:

$$V_{bus} = \sum_{i=1}^{N} V_{out,i} = \sum_{i=1}^{N} (k_i * V_{mpp}) = \left(n * k_n + m * k_m\right) * V_{mpp} = N * V_{mpp} * k_n * [\beta + \alpha * (1 - \beta)] \tag{20}$$

In order to enable all solar power generation modules in the system to work at their respective maximum power points, the range value of the DC bus voltage must be appropriately set. The required DC bus voltage is the minimum and maximum, as shown below:

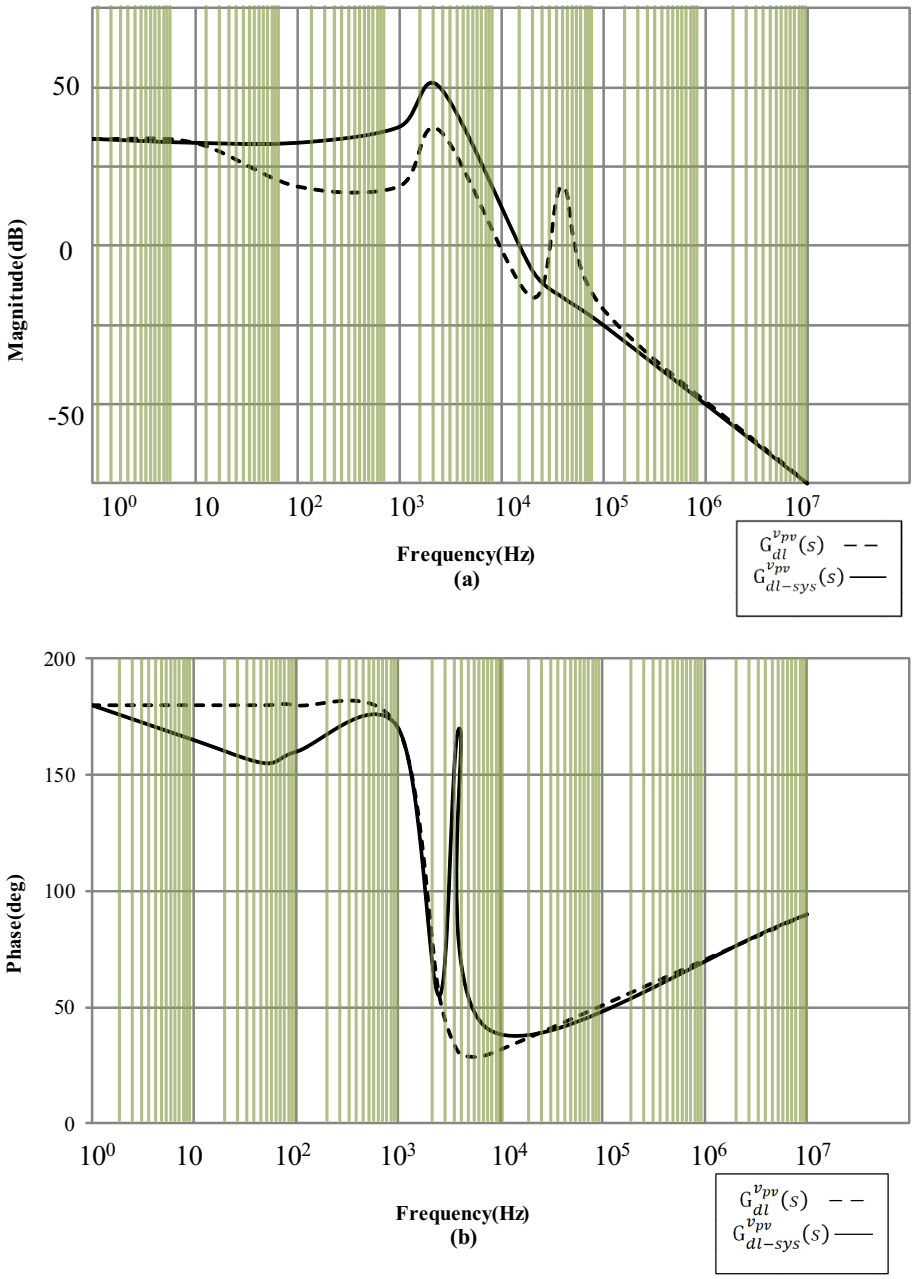

Fig. 5 Bode plot of current loop in boost mode

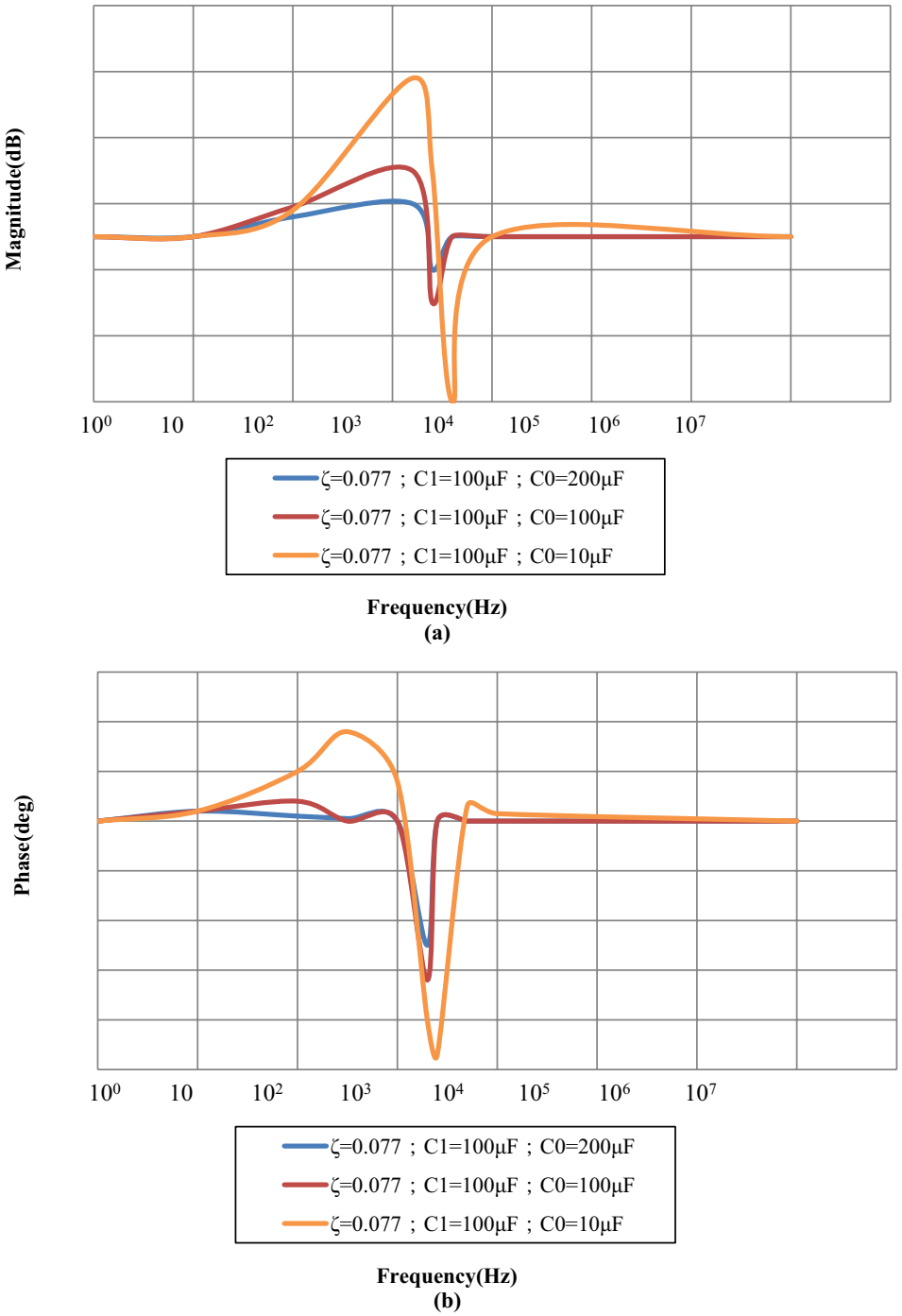

Fig. 6 Bode plot of voltage loop in boost mode

$$V_{bus\_min} = N * V_{mpp} * k_{min}[\frac{\beta}{\alpha} + (1-\beta)] \quad (21)$$

$$V_{bus\_max} = N * V_{mpp} * k_{max}[\frac{\beta}{\alpha} + (1-\beta)] \quad (22)$$

If you want to make full use of the energy of all solar power modules in the system, as shown below:

$$\alpha > k_{min}/k_{max} \quad (23)$$

As shown in Fig. 5, the zero on the left half plane provides enough phase margin for the current loop PI regulator, and G_{ic} simply adjusts the bandwidth of the current loop. The fault frequency of the current loop is set to one-tenth of the switching frequency.

Shown in Fig. 6 is a function of external voltage. It can be seen from Fig. 6 that the compensated transfer function has a better suppression effect on the inherent 100 Hz voltage ripple of the output voltage. In other words, the LoopHz ripple that exceeds the input voltage of the power arithmetic unit can be greatly reduced by the control loop to reduce the influence on the judgment of the direction of the external interference of the MPPT.

4 Practical application of output power optimization control of unipolar photovoltaic grid-connected micro-inverter

4.1 Power optimizer parameter design

The cascaded Buck/Boost circuit structure is very simple. The main passive components include inductor L, input capacitor, and output capacitor. When the power oscilloscope is running in the step-down mode, the induced current can be expressed as follows:

$$\Delta I_{Lboost} = (V_{pv} - V_{out})/LD_{boost}T_{sw} = V_{pv}(1 - D_{buck})/L* D_{buck}T_{sw} \tag{24}$$

The inductor current when the power optimizer works in Boost mode can be expressed as:

$$\Delta I_{Lboost} = \frac{V_{pv}}{L} * D_{boost}T_{sw} \tag{25}$$

In the boost mode, the inductor current ripple is larger than in the Buck mode, so the inductor current ripple becomes larger in the boost mode. In order to continuously maintain the current of the rising mode inductor, the inductor L must meet the following conditions:

$$L \geq \frac{V_{mpp}^2}{2P_{in,min}} * D_{boost,max}T_s \tag{26}$$

Here $P_{in,min}$ is the minimum input power of the startup mode, and $D_{boost,max}$ is the maximum duty cycle of the startup mode. The increase of the inductance helps reduce the fluctuation of the inductor current, but the excessive inductance value affects the dynamic response of the circuit and increases the volume and cost of the circuit. Therefore, compromise points need to be considered. The fluctuation of the input voltage depends on the size of the input capacity G. As follows:

$$C_{in} \geq I_{mpp}/\Delta V_{pv}(1 - D_{buck,min})T_{sw} \tag{27}$$

Here I_{mpp} is the maximum power point current of the solar cell module at rated power, and $D_{buck,min}$ is the minimum duty cycle in the stable state in the post mode. For the same reason, the ripple of the output capacitor in the startup mode becomes larger, so it is as follows:

$$\Delta V_{out} = \frac{I_{out}}{C_0} * D_{boost}T_{sw} = I_{mpp}/C_0(1 - D_{boost})D_{boost}T_{sw} \tag{28}$$

When D_{boost}=0.5, the above equation reaches the maximum value, so the minimum value of the output capacity of the power calculator is as follows:

$$C_0 \geq I_{mpp}/\Delta V_{out} * 0.25T_{sw} \tag{29}$$

The increase of input capacity and output capacity is beneficial to reduce the fluctuation of input and output voltage, but the increase of capacity has a great influence on the dynamic characteristics of solar cell maximum power tracking. The final switching frequency is selected as 200 kHz, the input capacity and output capacity are $63\mu F$ and $220\mu F$ respectively, and the inductance is $50\mu H$.

Table 1 Maximum power tracking experiment results

Experiment	1	2	3	4	5	6	7
Rated output power (W)	500	600	700	800	600	500	300
Power output voltage UI (V)	350	320	350	430	340	690	780
Power output current I (A)	2.8	2.9	2.3	2.5	2.6	2.7	2.8
Thermal resistance R (ohm)	60.1	40.5	50.6	60.6	70.8	25.6	23.4
Output voltage U2 (V)	178	152	143	156	157	178	179
Theoretical maximum power PI (W)	508	509	508	600	670	550	530
Actual input voltage P (W)	508	697	906	789	1102	1103	550
Maximum power tracking efficiency n (%)	99	98	99	99	99	98	99

Table 2 Inverter grid-connected experiment test record table

Experiment	Output power (W)	500	700	900	1100	1300	1500	1700
1700 W experimental prototype	Effectiveness(%)	91	92	92	91	91	93	91
	Power factor	0.9	0.9	0.9	0.8	0.7	0.6	0.8
	THD (%)	5.6	5.7	5.8	5.9	6.7	6.8	6.6
SMA SB1700	Effectiveness(%)	92	93	94	95	96	94	93
	Power factor	0.9	0.8	0.9	0.8	0.9	0.7	0.8
	THD (%)	7	5	7	8	9	6	5

Table 3 Unipolar and bipolar efficiency

Power (W)	500	700	900	1100	1300	1500	1700
Unipolar efficiency	91	92	92	91	92	91	92
Bipolar efficiency	87	89	90	89	87	88	89

4.2 Maximum power tracking test

In order to quantitatively test the tracking effect, we simulated the solar panel in series with a stable power supply and an adjustable resistance R. The MPPT voltage is different from the standard panel, but the output characteristics can fully verify the MPPT characteristic curve, avoiding errors caused by changes in the resistance value caused by the influence of electric power.

According to the analysis of the above circuit, when the inverter wants to obtain the maximum power from the DC power supply, the input voltage of the inverter needs to be adjusted to track half of the power supply voltage, as shown in Table 1:

It can be seen from Table 1 that the maximum power tracking efficiency obtained by the experiments of each group shows that the maximum power tracking efficiency of the inverter has reached more than 99%, and the inverter can effectively track the maximum power point.

4.3 Grid-connected inverter experiment analysis

The main indicators to verify the performance of the inverter are efficiency, power, and THD. The efficiency is the output power of the inverter divided by the input power of the inverter, which reflects the solar energy utilization rate of the solar power grid-connected inverter. The power factor represents the performance of the grid-connected current for synchronously tracking the grid voltage. When the power factor is 1, it means that the grid-connected current and the grid voltage are at exactly the same frequency and phase. THD refers to the ratio of the root mean square value of all harmonic components to the root mean square value of the fundamental wave, and indicates the degree of distortion of the grid-connected current. The lower the distortion rate, the better the performance.

Table 4 Passive island detection experimental data

P_R(W)	Q_L(Var)	Q_c(Var)	Grid voltage (V)	Grid frequency (Hz)	Error status
1700	1600	1600	220	55	Frequency out of bounds
	1600	1500	220	44	Frequency out of bounds
800	1600	1650	220	50	Grid overvoltage
2000			195	50	Grid undervoltage

The three main indicators of efficiency, power, and THD were tested and compared with the 1700 W grid-connected inverter of SMACompany, a technology leader in the field of solar power inverters, on the same experimental platform. The results are shown in Table 2:

It can be seen from Table 2 that the three main indexes of the system are not too far away from SMA. From the point of view of harmonic content and power factor, the index of this prototype is excellent. The efficiency comparison between the two is shown in Table 2. This is because the quality of overseas transformers has not reached the same level.

Power factor and THD indicate that the greater the power of the inverter, the better the grid-connected effect. The grid-connected current amplitude of the inverter increases with the increase of the output power, so the proportion of the harmonic components of the current in the current becomes smaller, and as the power increases, the THD will also decrease. In addition, when the inverter power is half of the rated power, the efficiency index is the highest, which may reach 92.49%.

Table 5 Island detection experiment data

Output Power		Reactive power	PR (W)	QL range (Var)		QC (Var)	Response time range (S)		Error status
100%	1700 W	20Var	1700	1600	1700	1600	0.3	1.7	Island state
60%	1100 W	30Var	1100	1100	1100	1030	0.5	1.8	Island state
33%	500 W	40Var	500	500	600	502	0.6	1.5	Island state

In order to verify the advantages of unipolar control, the system uses bipolar control for grid-connected experiments, and tests the efficiency of the inverter at each main power point. The comparison between the obtained data and the unipolar control is as follows:

It can be seen from Table 3 that the bipolar efficiency is 3% lower than the unipolar efficiency on average. In the unipolar control mode, the system loss is significantly reduced and the efficiency is significantly improved.

4.4 Island detection experiment

In order to simulate the passive islanding detection scheme, this experiment adjusted the RLC load so that the effective output power and reactive power of the inverter did not match. Next, cut off the power grid and read the effective value and frequency of the power. The grid voltage detected by the power quality analyzer. The experimental data obtained with the rated output of 1700 W is shown in Table 4 below:

As shown in Table 4, when the rated output is 1700 W, the reactive power output of the system is 20VAR. The effective power is insufficient, the output voltage is pulled down, and the system reports an error. According to the above data, if the output of the inverter is inconsistent with the power of the load, the system will report an error, and the connection to the power grid can be cut off.

The active island detection method designed in this paper is to perturb the output power to judge the state of the island. Passive island detection test platform can be used for active island detection test. The difference is that in order to detect the island detection performance of the system under extreme conditions, in the active island detection test, the effective power and reactive power of the load must be consistent with the output of the inverter. Therefore, the experimental steps are as follows:

In the test, the inverter is first adjusted according to the rated power output, the reactive power output is adjusted to Q, and then L is adjusted to make the reactive power $Q_L = P$ obtained by the load box from the power grid. Adjust C so that the load box receives reactive power $Q_C = P - Q$ from the grid. Adjust R to create the effective power that the load box draws from the grid.

First adjust the inductance to lower the harmonic components of the current, then install a capacitor, maintain the voltage while inserting a resistor, and finally insert a resistor to adjust.

The detection of the island is carried out near the equilibrium point, L is adjusted to add or subtract 5%, the load reactive power is adjusted 1% each, and the power will increase or decrease by 5%. After the system is stable, K2 is cut off, and the time until the inverter error is recorded.Adjust the output power of the inverter to 66% of the rated power and repeat the steps.Adjust the output power of the inverter to 33% of the rated power and repeat the steps. The experimental results obtained are shown in Table 5.

It can be seen from Table 5 that the island test tested 3 power points, and 11 sets of data were tested at each power point. The time range shown in the table is less than 2 s, indicating that the island detection method of the system meets the requirements.

5 Conclusion

Since the beginning of the 21st century, solar energy has four major advantages: continuous supply, clean and harmless, huge reserves, and convenient use. The energy consumption structure and new energy investment have gradually tilted toward solar power generation. This means that solar power technology is likely to become a breakthrough in China's energy problems. This article briefly introduces the main circuit structure of the single-phase single-row grid-connected inverter, compares the current optimization mode followed by the maximum power point and the voltage optimization mode, and establishes the mathematical model of the current output grid-connected inverter. Execute Simonk simulation in the system to verify its feasibility. Research based on dual current control and dual current control. The outer voltage loop is controlled by PI to ensure the stability of the bus voltage, and the inner current loop is controlled by quasi-proportional resonance. In this way, a specific current can be tracked without static error, and the influence of

grid voltage failure on system control can be reduced. Based on the previous control of the inverter's output unit power factor, a reactive power compensation control strategy for single-phase solar power inverters is proposed. Use instantaneous no-power theory to realize the effective power control and reactive power compensation of the inverter, and optimize the function of the inverter. The above-mentioned theoretical analysis and algorithm are all verified by the power electronic simulation software SABRE. Finally, the maximum power point following efficiency is obtained through physical experiments, which will prove the effectiveness of system power control.

Funding The study was supported by (1)The National Science and Technology Support program of China (Grant No.2015BAF20B02); (2)The Special Project of Shanxi Province Education Science "1331 Project" (Grant No.ZX-18050); (3)The Science Foundation for Youths of Shanxi Datong University (Grant No.2018Q7).

Data availability The data used to support the findings of this study are available from the corresponding author upon request.

Declarations

Conflict of interest The author(s) declare(s) that they have no conflicts of interest.

Informed consent Not applicable.

References

Abadie A, Diamond A, Hainmueller J (2010) Synthetic control methods for comparative case studies: estimating the effect of California's tobacco control program. J Am Stat Assoc 105(490):493–505

Balaguer IJ, Lei Q, Yang S et al (2010) Control for grid-connected and intentional islanding operations of distributed power generation. IEEE Trans Ind Electron 58(1):147–157

Barlev D, Vidu R, Stroeve P (2011) Innovation in concentrated solar power. Sol Energy Mater Sol Cells 95(10):2703–2725

Chiu CS (2010) TS fuzzy maximum power point tracking control of solar power generation systems. IEEE Trans Energy Convers 25(4):1123–1132

Fiaschi D, Bandinelli R, Conti S (2012) A case study for energy issues of public buildings and utilities in a small municipality: investigation of possible improvements and integration with renewables. Appl Energy 97:101–114

Guerrero JM, Blaabjerg F, Zhelev T et al (2010) Distributed generation: toward a new energy paradigm. IEEE Ind Electron Mag 4(1):52–64

Hill CA, Such MC, Chen D et al (2012) Battery energy storage for enabling integration of distributed solar power generation. IEEE Trans smart grid 3(2):850–857

Kabalcı E (2020) Review on novel single-phase grid-connected solar inverters: circuits and control methods. Sol Energy 198:247–274

Keshani M, Adib E, Farzanehfard H (2018) Micro-inverter based on single-ended primary-inductance converter topology with an active clamp power decoupling. IET Power Electron 11(1):73–81

Kouro S, Leon JI, Vinnikov D et al (2015) Grid-connected photovoltaic systems: an overview of recent research and emerging PV converter technology. IEEE Ind Electron Mag 9(1):47–61

Kumar VP, Fernandes BG (2017) A fault-tolerant single-phase grid-connected inverter topology with enhanced reliability for solar PV applications. IEEE J Emerg Sel Top Power Electron 5(3):1254–1262

Kumari J, Babu CS (2012) Mathematical modeling and simulation of photovoltaic cell using matlab-simulink environment. Int J Electr Comput Eng 2(1):26

Pfenninger S, Hawkes A, Keirstead J (2014) Energy systems modeling for twenty-first century energy challenges. Renew Sustain Energy Rev 33:74–86

Rezaei MA, Lee KJ, Huang AQ (2015) A high-efficiency flyback micro-inverter with a new adaptive snubber for photovoltaic applications. IEEE Trans Power Electron 31(1):318–327

Schot J, Kanger L, Verbong G (2016) The roles of users in shaping transitions to new energy systems. Nat energy 1(5):1–7

Wang Q, Zhang C, Wu X et al (2019) Commutation failure prediction method considering commutation voltage distortion and DC current variation. IEEE Access 7:96531–96539

Wu JC, Chou CW (2013) A solar power generation system with a seven-level inverter. IEEE Trans Power Electron 29(7):3454–3462

Yaqoob SJ, Obed A, Zubo R et al (2021) Flyback photovoltaic microinverter with a low cost and simple digital-analog control scheme. Energies 14(14):4239

Zhao ZY, Chen YL (2018) Critical factors affecting the development of renewable energy power generation: evidence from China. J Clean Prod 184:466–480